Dynamics in electron transfer protein complexes

Bashir, Q.

Chapter 3

Binding hot spot in the weak protein complex of cytochrome *c* and cytochrome *c* peroxidase

This work has been published as part of

Volkov AN, Bashir Q, Worrall JA & Ubbink M. Binding hot spot in the weak protein complex of physiological redox partners yeast cytochrome *c* and cytochrome *c* peroxidase. *J Mol Biol* **385**, 1003-13 (2009).

Thesis: Dynamics in Electron Transfer Protein Complexes
Qamar Bashir, 2010

Addendum to the Acknowledgements

I would like to acknowledge Dr. Alexander Volkov for his important contribution to chapter 3. He performed the mutagenesis and the protein production of cytochrome c and analyzed the data. I produced cytochrome c peroxidase and we recorded the titrations together.

Qamar Bashir

Abstract

Transient protein interactions mediate many vital cellular processes such as signal transduction or intermolecular electron transfer. However, due to difficulties associated with their structural characterization, little is known about the principles governing recognition and binding in weak transient protein complexes. In particular, it has not been well established whether binding hot spots, which are frequently found in strong static complexes, also govern transient protein interactions. To address this issue, we have investigated an electron transfer complex of physiological partners from yeast: yeast iso-1-cytochrome *c* (Cc) and yeast cytochrome *c* peroxidase (CcP). Using NMR spectroscopy, we show that Cc R13 is a hot-spot residue, as R13A mutation has a strong destabilizing effect on binding. Furthermore, we employ a double-mutant cycle to demonstrate that Cc R13 interacts with CcP Y39. The present results, in combination with those of earlier mutational studies, have enabled us to outline the extent of the energetically important Cc–CcP binding region. Based on our analysis, we propose that binding energy hot spots, which are prevalent in static protein complexes, could also govern transient protein interactions.

Introduction

Interactions between proteins mediate most cellular functions. The variation in the strengths of protein–protein complexes is staggering. The corresponding dissociation constants span a range of 14 orders of magnitude.[11,12] At one extreme of this continuum are tight (nanomolar to subpicomolar), long-lived, highly specific complexes (e.g., those of antigens and antibodies, or enzymes and inhibitors), which we refer to as "static" in this work. At the other end of the scale are weak (millimolar to micromolar) short-lived complexes formed by proteins that recognize multiple partners. These interactions, referred to as "transient," orchestrate biochemical transmission processes such as those taking place in signal transduction cascades or electron transfer (ET) chains.

Despite their functional importance and because of difficulties associated with their structural characterization, weak transient complexes are largely underrepresented in published analyses of protein interfaces.[127-132] As a consequence, the present understanding of the principles underlying protein-protein recognition and binding comes almost exclusively from the study of static complexes. It has been shown that many factors that are believed to determine binding strength in static complexes (such as shape complementarity, interface size, and specific intermolecular contacts) are much less important for transient ones.[14,111] This raises a question of how much of what we have learned from static complexes holds true for their transient counterparts. In particular, it would be interesting to know whether binding hot spots, which are frequently found in static complexes,[129,132-135] also govern transient protein interactions.

In a seminal alanine scanning mutagenesis study of human growth hormone binding to its receptor, Clackson and Wells showed that only a few surface residues on both proteins are energetically important for the interaction.[136] These are clustered together in an interface region, aptly named "hot spot," and surrounded by residues whose replacement by alanine has a small or no effect on binding energy. A further analysis of hot spots in protein-protein complexes has shown that, as a rule, those are located in the center of the interface and enriched in tryptophan, tyrosine, and arginine groups.[129] Furthermore, it was demonstrated that hot-spot residues defined as those increasing the binding free energy of the complex by $\geq$2 kcal mol^{-1} upon mutation to alanine constitute on average only ~10% of all interfacial residues.[132] At present, it is not clear whether

binding hot spots orchestrate transient protein interactions; to the best of our knowledge, these have been reported for only one weak complex (K_d ~ 2 μM).[137] Interestingly, analysis of transient ET protein complexes reveals that their binding site architecture is highly suitable for hot spots, with an enhanced hydrophobic environment at the center of the interface, charged residues at the periphery, and interface enrichment in arginine residues.[111]

Despite having been extensively studied in the past several decades, the yeast iso-1-cytochrome *c* (Cc)–yeast cytochrome *c* peroxidase (CcP) complex remains a popular system for the investigation of biomolecular ET.[138,139] The Cc–CcP crystal structure has been solved,[81] and a paramagnetic relaxation enhancement NMR study has established that the protein–protein orientation observed in the crystal is indeed the dominant form of the complex in solution.[19] In the crystal, the Cc–CcP interaction comprises multiple van der Waals contacts and a single intermolecular hydrogen bond (Cc N70–CcP E290; Figure 3.1a). The small (1150 $Å^2$) binding interface is formed by residues surrounding the haem group of Cc and located near V197 and Y39 on CcP (Figure 3.1b and c). Upon binding, R13 of Cc and Y39 of CcP (Figure 3.1b and c, green) lose 67 $Å^2$ and 107 $Å^2$ of their solvent-accessible surface areas (SASAs), respectively, which makes them the most buried residues in the interface. Arginine and tyrosine are two of the most frequent hot-spot residues[129] and are commonly found in the binding sites of redox protein complexes.[111]

Surrounded by a shell of atoms making van der Waals contacts with the partner protein, R13 of Cc sits in the middle of the interface (Figure 3.1b). Its central position and a likely occlusion from the solvent make R13 a prime candidate for a binding hot spot in the Cc–CcP complex. Similarly, CcP residue Y39, which makes an intermolecular contact with R13 of Cc (Figure 3.1a), could be part of the corresponding hot spot on CcP.

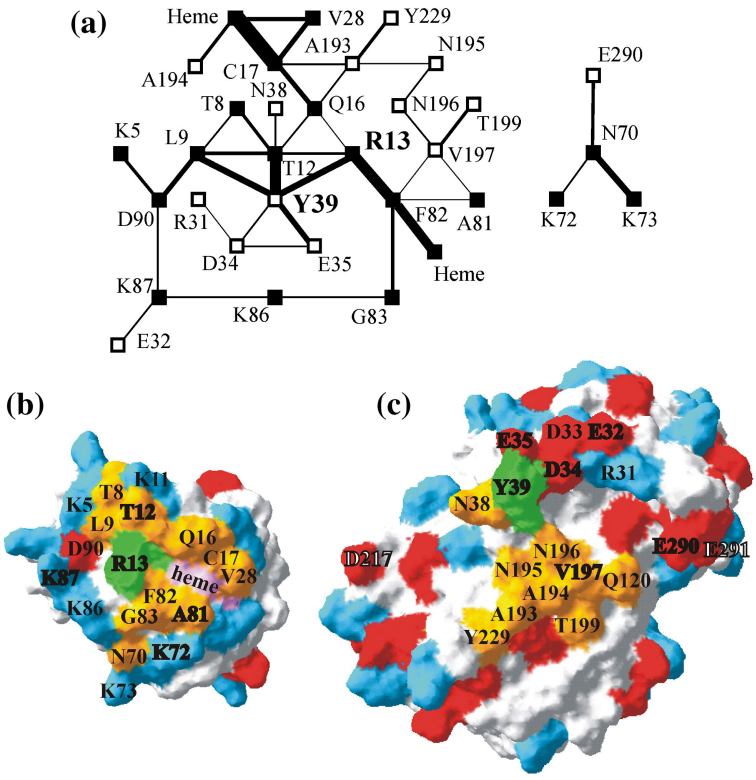

Figure 3.1. Cc–CcP binding interface as seen in the crystal structure (PDB entry 2PCC).[81] (a) Cc–CcP contact map. Filled and open squares denote Cc and CcP residues, respectively. The legitimate noncovalent interatomic contacts between interface residues have been identified and analyzed using the CSU software,[140,141]. The analysis was performed by Dr Alexander Volkov. The lengths of the lines connecting the nodes are arbitrary, while their widths denote the strengths of the interactions. Enlarged labels indicate the most buried Cc and CcP residues in the interface: R13 and Y39, respectively. (b and c) Binding surfaces of (b) Cc and (c) CcP. Negatively and positively charged residues are shown in red and blue, respectively. The amino acids that lose SASA upon complex formation are coloured and indicated by filled labels. Cc haem group is shown in pink. The two most buried interface residues investigated in this study are shown in green. Bold and open labels identify, respectively, the residues located within and outside of the crystallographically defined binding site, and for which the effects of mutations on K_B are known from this and earlier studies.

Using NMR spectroscopy, we show that R13A mutation of Cc has a strong destabilizing effect on binding, while the effect of Y39A CcP substitution is a little less pronounced. In addition, double-mutant cycle analysis confirms that the Cc R13–CcP Y39 interaction stabilizes the protein complex. Together with the results of earlier

mutational studies,[142,143] these findings enable us to outline the extent of the energetically important Cc–CcP binding region.

Materials and Methods

Protein preparation

Both native and ^{15}N-labelled wt Cc were expressed in *Escherichia coli* and purified as previously described.[112,144] The wt CcP was isolated from *E. coli* following published procedures.[145] The mutations studied in this work were introduced by site-directed mutagenesis using the Quik Change™ polymerase chain reaction protocol (Stratagene, La Jolla, CA), with the corresponding wt plasmid as template. All constructs were verified by DNA sequencing, and the mutants were expressed and purified analogously to the wt proteins. Throughout the study, we used ferric Cc and high-spin ferric CcP with previously reported purity criteria.[101] Concentrations of Cc and CcP were determined from UV–Vis spectra using $\varepsilon_{410\ nm}$=106.1 mM^{-1} cm^{-1} and $\varepsilon_{408\ nm}$=98 mM^{-1} cm^{-1}, respectively.[101]

NMR spectroscopy

We have used 0.8 - 1.0 mM free ^{15}N wt Cc and 0.5 mM of its 1:1 complexes with wt or Y39A CcP for chemical shift perturbation analysis. To obtain the binding constants by NMR, 0.5 mM wt or Y39A CcP was titrated with a concentrated stock (1.7-2.2 mM) of wt or ^{15}N R13A Cc. All NMR samples contained 20 mM sodium phosphate, 100 mM NaCl (pH 6.0), and 6% D_2O for lock. In addition, the samples used for 1D ^{1}H or 2D [^{15}N,^{1}H] HSQC experiments contained, respectively, 0.1 mM 3- (trimethylsilyl)-propionic acid-D4 (sodium salt) or ^{15}N acetamide as internal reference. The pH of the samples was adjusted to 6.00±0.05, with small aliquots of 0.1 M HCl or NaOH. Measurements were performed at 303 K on a Bruker DMX600 spectrometer equipped with a TCI-Z-GRAD CryoProbe (Bruker). One-dimensional ^{1}H spectra with a soft presaturation pulse for water suppression were acquired with a spectral width of 70 ppm and 4096 points. Two-dimensional [^{15}N,^{1}H] HSQC spectra with a water-gate pulse[146] for water suppression were obtained with 512 and 128 complex points in the direct and

indirect dimensions, respectively. For backbone amide experiments, the spectral widths in ^{15}N and ^{1}H dimensions were 42 ppm and 16 ppm, respectively, with a ^{15}N offset of 119 ppm. For observation of the R13 side-chain amide, the spectral width and the offset in ^{15}N dimension were 70 ppm and 113 ppm, respectively.

All data were processed with Azara 2.7 (http://www.bio.cam.ac.uk/azara/) and analyzed in Ansig for Windows.[115] Assignments of the HSQC spectra of the free and bound ^{15}N wt Cc were taken from a previous report.[101] The HSQC spectrum of ^{15}N R13A Cc was identical to that of ^{15}N wt Cc, except for several resonances of the residues around the mutation site, and was assigned unambiguously using 3D NOESY-HSQC and 3D TOCSY-HSQC experiments. The average amide chemical shift perturbations ($\Delta\delta_{avg}$) were derived from Eq. (3.1):

$$\Delta\delta_{avg} = \sqrt{\frac{\left(\Delta\delta^{N}/5\right)^2 + \left(\Delta\delta^{H}\right)^2}{2}} \tag{3.1}$$

where $\Delta\delta^{N}$ and $\Delta\delta^{H}$ are the chemical shift perturbations of the amide nitrogen and proton, respectively. With the derived binding constants it was calculated that 90% and 77% wt Cc are bound to wt and Y39A CcP, respectively, at the protein concentrations used in the chemical shift perturbation experiments. In order to obtain $\Delta\delta_{avg}$ extrapolated to the 100% bound form, the respective $\Delta\delta_{avg}$ values were divided by 0.9 or 0.77.

NMR chemical shift titration curves were analyzed with a two-parameter nonlinear least squares fit using a one-site binding model (Eq. (3.2)):

$$\Delta\delta = \tfrac{1}{2}\Delta\delta_0\left[A - \sqrt{A^2 - \frac{4}{R}}\right] \tag{3.2a}$$

$$A = 1 + \tfrac{1}{R} + \frac{[Cc]_0 + R[CcP]_0}{R[Cc]_0[CcP]_0 K_B} \tag{3.2b}$$

where $\Delta\delta$ is the chemical shift perturbation at a given protein ratio; $\Delta\delta_0$ is the chemical shift perturbation at 100% Cc bound; R is the [Cc]/[CcP] ratio at a given point; $[Cc]_0$

and $[CcP]_0$ are the concentrations of Cc stock solution used for the titration and the CcP starting solution, respectively; and K_B is the binding constant of the complex. Thus, $\Delta\delta$ and R are the dependent and independent variables, respectively, and $\Delta\delta_0$ and K_B are the fitted parameters.

Double-mutant cycles

The coupling energy parameter $\Delta\Delta G_c$ was calculated using Eq. (3.3):[143,147]

$$\Delta\Delta G_c = \Delta G_{X,Y} - \Delta G_{X\to A,Y} - \Delta G_{X,Y\to A} + \Delta G_{X\to A,Y\to A} \qquad (3.3)$$

where X and Y represent the wt residues of Cc and CcP, respectively, and A symbolizes a mutation to alanine. Uncertainties were estimated using standard error propagation procedures.

Ring current shifts

The ring current shift (δ_{rc}) of the Cc R13 H^{ε} nucleus was calculated from Eq. (3.4):

$$\delta_{rc} = iBG(r) \qquad (3.4)$$

where i is the intensity factor, B is a constant, and G(r) is a geometric factor. The values of i =1.24 and B=5.445 × 10^{-6} Å were taken from the literature,[148] and G(r) was calculated using the Haigh–Mallion model (Eq. (5)):[149]

$$G(r) = \sum_{ij} s_{ij}\left(\frac{1}{r_i^3} + \frac{1}{r_j^3}\right) \qquad (3.5)$$

where r_i and r_j are the distances from ring atoms i and j to the proton, and s_{ij} is the signed area of the triangle formed by atoms i and j and the proton projected onto the plane of the aromatic ring. The sum is over the bonds of the ring. To calculate the geometric factor, the coordinates of Cc R13 and CcP Y39 side chains were taken from

the crystal structure of the complex (PDB entry 2PCC),[81] to which hydrogen atoms had been added in Xplor-NIH.[150] The ring current shifts were calculated for both complexes in the asymmetric unit (protein chains A and B, and protein chains C and D).

Results

Cc–CcP contact map

Following the work of Reichmann et al., we have constructed the Cc–CcP interaction map[141,151] (Figure 3.1a). The resulting contact map shows that although both proteins bury equal amounts of SASA upon complex formation (ca 570 $Å^2$ each), the interactions of Cc side chains are more extensive (Figure 3.1a). On the CcP side, most of the interactions are clustered around several residues, one of which (Y39) could make as much as five intermolecular and intramolecular contacts with its interface neighbors (Figure 3.1a).

Binding parameters obtained from NMR

To explore the role of putative hot-spot residues Cc R13 and CcP Y39 in Cc–CcP complex formation, we have studied the binding of R13A Cc and Y39A CcP variants. The binding parameters for the mutant complexes are combined in Table 3.1. To measure the binding constants NMR titrations were performed. In each case, chemical shift perturbations of Cc resonances are followed as Cc is titrated into CcP (Figure 3.2). As the Cc–CcP complex is in fast exchange on the NMR chemical shift time scale,[101] a single set of Cc peaks is observed throughout the titration. Binding of wt Cc to Y39A CcP was followed in a series of one-dimensional (1D) ^{1}H NMR spectra by monitoring the changes in the position of a downfield hyperfine-shifted Cc haem resonance (Figure 3.2a). For R13A Cc–CcP complexes, chemical shift perturbations of ^{15}N R13A Cc backbone amide resonances were monitored in a series of two-dimensional (2D) [^{1}H,^{15}N] heteronuclear single quantum coherence (HSQC) spectra (Figure 3.2b and c). The data were fitted to a 1:1 binding model (Eq. 3.2) and the binding constants were calculated (Table 3.1).

Table 3.1. Cc–CcP binding parameters

	K_B [a]	ΔG_B (kcal mol^{-1})
	wt CcP	
wt Cc [b]	20	− 7.3
R13A Cc	0.6 ± 0.2	− 5.2 ± 0.2
	Y39A CcP	
wt Cc	1.4 ± 0.3	− 5.7 ± 0.1
R13A Cc	0.57 ± 0.02	− 5.2 ± 0.1

Experiments were performed in 20 mM sodium phosphate and 0.1 M NaCl (pH 6.0) at 303 K. The uncertainties are the standard errors of the fit for NMR data.

[a] Equilibrium binding constant in units of 10^4 M^{-1}.

[b] Lower limit of the binding constant taken from previous work.[101]

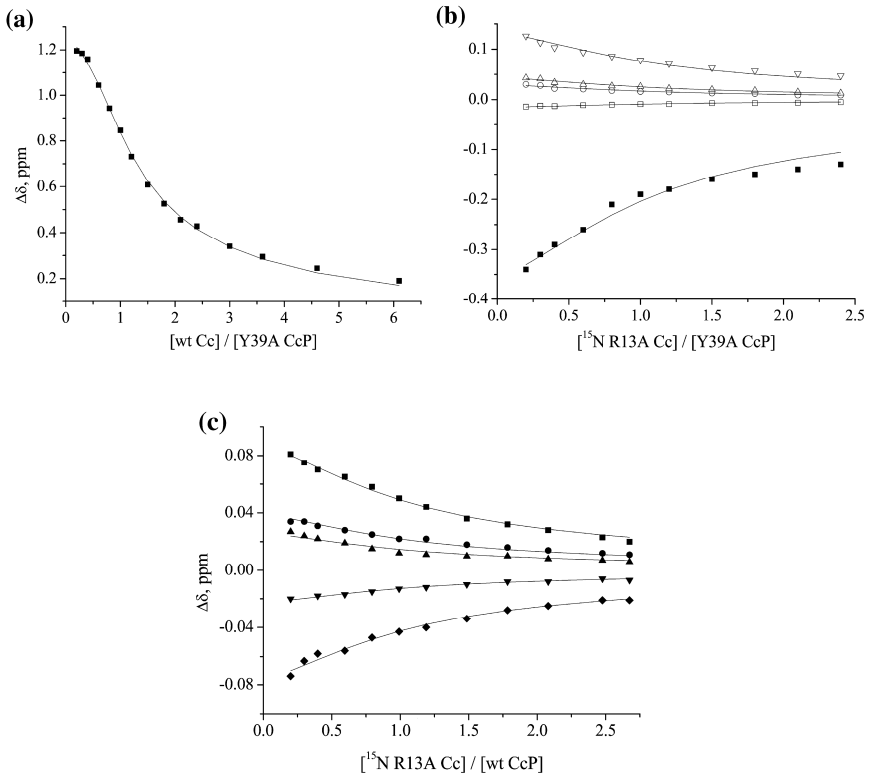

Figure 3.2. NMR titrations of (a) wt and (b) R13A Cc with Y39A CcP, and of (c) R13A Cc with wt CcP. (a) Binding shifts of the downfield shifted Cc haem 3-CH_3 resonance followed in 1D ^{1}H NMR spectra. The solid line represents the best fit to a 1:1 binding model. (b and c) Two-dimensional [^{1}H,^{15}N] HSQC binding shifts of the H^N (open symbols) and N^H (filled symbols) atoms of ^{15}N R13A Cc upon binding to (b) Y39A CcP or (c)

wt CcP. The titrations curves are shown for R13A Cc residues: (b) K5 (circles), L9 (triangles), G77 (inverted triangles), and T78 (squares); and (c) A7 (triangles), L9 (squares), T78 (inverted triangles), F82 (diamonds), and D90 (circles). Solid lines in (b) and (c) show the best simultaneous fit of the curves to a 1:1 binding model with a shared K_B value (Eq 3.2). The obtained binding parameters and experimental conditions are given in Table 3.1.

Double-mutant cycle

For two interacting proteins, double-mutant cycles allow the identification of pairs of residues whose side chains form stabilizing intermolecular contacts.[147,152,153] To this end, each residue is substituted by an alanine, and the effects of the mutations on binding are measured. Noncooperativity of the effects of the two mutations (i.e., the change in free energy for the double mutant is the sum of free energies for the two single mutations) indicates that either the two residues do not interact or their interaction does not contribute to the binding energy. But if the effects are coupled (i.e., the change in free energy for the double mutant differs from the sum of free energies for the two single mutants), then the mutated residues must form an intermolecular contact affecting the stability of the protein complex. The coupling energy ($\Delta\Delta G_c$), which is a measure of the cooperativity of interaction,[152] can be computed from Eq. 3.3,.[143,147] using the NMR binding constants given in Table 3.1, yielding $\Delta\Delta G_c = -1.6 \pm 0.3$ kcal mol^{-1} for the Cc R13–CcP Y39 pair. This value indicates that the interaction between Cc R13 and CcP Y39 stabilizes the complex.

NMR chemical shift perturbations

As mentioned above, the interaction between an isotopically labelled protein and its unlabelled partner can be conveniently followed by heteronuclear 2D NMR spectroscopy. For instance, some of the [^{1}H,^{15}N] HSQC resonances of a ^{15}N-labelled protein change their positions upon binding to an unlabelled target, which can be used to map the interacting protein surfaces.[154] For the wt Cc–Y39A CcP complex investigated in this study, the binding shifts extrapolated to 100% Cc bound ($\Delta\delta_{avg}$; see Materials and Methods) are plotted in Figure 3.3. Overall, the $\Delta\delta_{avg}$ values for the C*c*–Y39A CcP are smaller than those for Cc–wt CcP. Despite the decrease in $\Delta\delta_{avg}$, the

chemical shift perturbation profiles for the two complexes are very similar (Figure 3.3), indicating that the same Cc residues are affected by binding to both wt and Y39A CcP. Weak transient protein–protein interactions can be conveniently described by a two-step binding model, according to which the dominant single-orientation complex is in equilibrium with a dynamic encounter complex consisting of multiple protein–protein orientations.[14,19,155] As emerges from the study of transient interactions in our group, the reduction in the size of $\Delta\delta_{avg}$ signifies a shift towards the encounter complex.[26,29,30,124,155] Thus, the decrease in $\Delta\delta_{avg}$ for Cc–Y39A CcP suggests that the proteins spend more time in search of the dominant binding geometry within this complex.

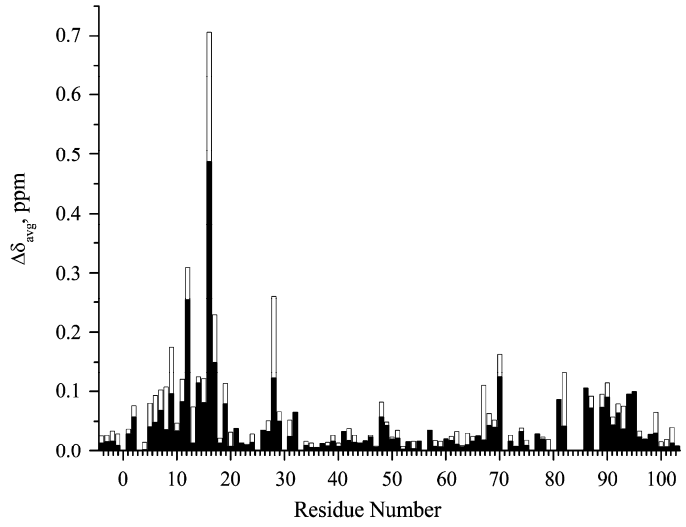

Figure 3.3. Chemical shift perturbation analysis of the wt Cc–Y39A CcP complex in solution. Filled and open bars show $\Delta\delta_{avg}$ for the binding of wt Cc to Y39A and wt CcP, respectively, at 303 K in 20 mM sodium phosphate and 0.1 M NaCl (pH 6.0). The values of $\Delta\delta_{avg}$ are extrapolated to 100% bound form (see Materials and Methods).

Interaction of Cc R13 and CcP Y39 side chains

Similarly to backbone amides, N^{ε} and H^{ε} nuclei of arginine side chains give rise to NMR signals in 2D [^{1}H,^{15}N] HSQC experiments. In addition to R13, yeast Cc contains two more arginines (R38 and R91), and the NH^{ε} peaks of all three residues are observed in the HSQC spectrum of the wt protein (Figure 3.4a). By recording the spectrum of

R13A Cc and by comparing it to that of the wt Cc, we were able to unambiguously assign the R13 NH^{ε} resonance of the wt protein (δ^{H}=7.031 ppm; δ^{N} =83.09 ppm).

The R13 side-chain amide of Cc is strongly affected by binding to the wt CcP (Figure 3.4a). The chemical shift perturbations extrapolated to 100% form ($\Delta\delta_0$; see Materials and Methods) are 0.704 ppm and 0.96 ppm for the proton and nitrogen nuclei, respectively. At the same time, interaction with Y39A CcP results in smaller binding shifts ($\Delta\delta_0^{H}$ = 0.148 ppm; $\Delta\delta_0^{N}$ = 0.82 ppm). The difference in the size of $\Delta\delta_0$ upon binding to wt and Y39A CcP is especially prominent along the proton dimension (Figure 3.4a), with $\Delta\Delta\delta_0^{H}$ = $\Delta\delta_0^{H}$ (Cc–wt CcP)–$\Delta\delta_0^{H}$(Cc–Y39A CcP)= 0.556 ppm. Inspection of the crystal structure of the wt complex fails to reveal a structural cause for such a large difference in binding shifts. As can be seen from Figure 3.4b, the NH^{ε} group of Cc R13 is too far from the CcP surface to either make a direct intermolecular contact or experience a significant ring current effect exerted by the aromatic ring of CcP Y39. Indeed, the ring current shift for the R13 H^{ε} nucleus calculated from the crystallographic side-chain coordinates is close to zero (−0.048 ppm and −0.074 ppm for the two complexes present in the asymmetric unit; see Materials and Methods). The large $\Delta\delta_0$ values observed for Cc R13 H^{ε} upon interaction with wt, but not with Y39A CcP, most likely reflect a difference in the binding-induced solvation changes of the Cc R13 group in the two complexes.

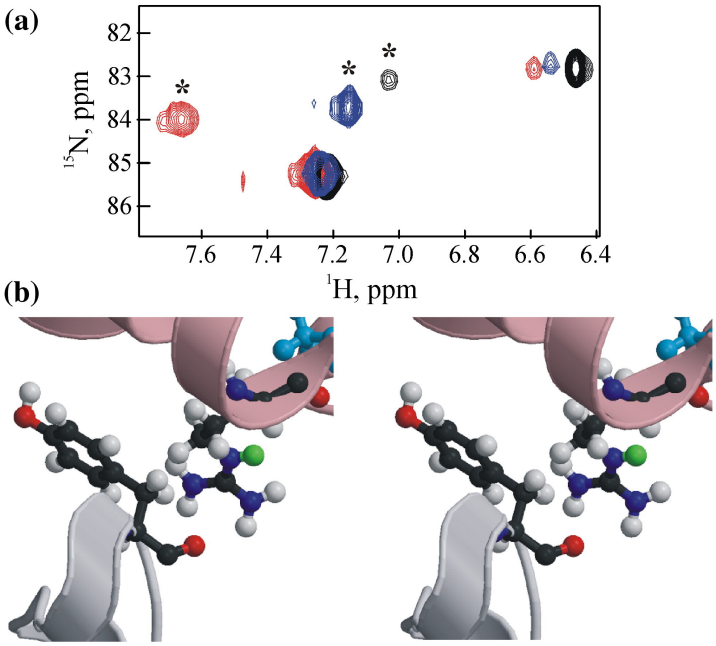

Figure 3.4. The interaction between Cc R13 and CcP Y39. (a) [^{1}H,^{15}N] HSQC resonances of NH$^{\varepsilon}$ arginine groups of ^{15}N Cc free (black) and in complex with wt CcP (red) or Y39A CcP (blue). Asterisks indicate R13 NH$^{\varepsilon}$ peaks. (b) Stereo view of Cc R13 and CcP Y39 side chains as seen in the crystal structure of the complex (PDB entry 2PCC).[81] The ribbon representations of Cc and CcP are shown in magenta and gray, respectively. Part of the Cc loop comprising residues 82–87 has been removed for clarity. The Cc haem group (cyan) and the side chains in question are shown in ball-and-sticks representation. The added hydrogen atoms are shown as light gray spheres, and Cc R13 H$^{\varepsilon}$ atom is shown in green. The image in (b) was made with MOLSCRIPT[156] and Raster3D.[157]

Discussion

Cc–CcP binding hot spot

The architecture of the Cc–CcP interface satisfies several important requirements for binding hot spots. On the Cc side, the contact surface is composed of a central core, surrounded by a ring of lysines (Figure 3.1b). The observed enhanced hydrophobic environment of the central patch and the presence of an arginine side chain (R13) in the middle of the binding surface are common features of both redox protein complexes[111] and binding hot spots.[129,132] On the CcP side, the interface consists of two patches

located around A194 and D34, and is composed of predominantly hydrophobic and negatively charged amino acids, respectively (Figure 3.1c). Joining the two patches is a tyrosine group (Y39), yet another ubiquitous hot-spot residue.[129,132] Also for the CcP interface, the presence of the hydrophobic core and a polar periphery seems to favor a binding hot spot.

Cc R13 and CcP Y39 are the two most buried amino acids in the interface and are likely the binding anchors[158] in the Cc–CcP complex. As we have shown above, substitution of either CcP Y39 or Cc R13 by an alanine leads to the weakening of the Cc–CcP interaction. While the former results in a moderate change in binding energy ($\Delta\Delta G_B$=1.6 kcal mol^{-1}), the latter has a larger destabilizing effect on the complex ($\Delta\Delta G_B$=2.1 kcal mol^{-1}). Thus, our results show that R13 of Cc is indeed a hot-spot residue.

As a rule, hot-spot regions of interacting proteins are complementary (i.e., the binding hot spot on one protein packs against that on the other).[129,132,136] In this regard, the moderate effect of Y39A CcP mutation which abolishes the interaction with Cc R13 and eliminates weak van der Waals contacts with Cc L9 and T12 (Figure 3.1a) is somewhat puzzling. One explanation for this behavior could be a structural rearrangement in the Cc–Y39A CcP complex. Unfortunately, due to weak binding and increased dynamics, solving the Cc–Y39A CcP structure by X-ray crystallography is a challenging task. Furthermore, paramagnetic relaxation enhancement NMR spectroscopy, which was applied successfully to the wt complex,[19] cannot be used to elucidate the solution structure of such highly dynamic protein–protein system because the paramagnetic effects arising from the well-defined form and the highly populated dynamic state of the complex can no longer be separated.[36] However, the similarity of the chemical shift perturbation profiles for Cc bound to wt and Y39A CcP suggests that the latter mutation does not perturb the overall structure of the protein complex. Rather, it seems more likely that slight reorientation of the Cc R13 side chain brings it into contact with other neighboring CcP residues (e.g., D34 or N196; see Figure 3.1c), thereby counterbalancing the destabilizing effect of Y39A substitution. Alternatively, the space vacated by the CcP Y39 side chain can now be occupied by one or more water molecules whose interaction with Cc R13 could restore binding.

In order to define hot-spot regions on the Cc–CcP interface, we have combined our data with those of previous mutagenesis studies (Table 3.2).[142,143] CcP is known to bind Cc at more than one site; however, at the high ionic strength used in this study (I=125 mM), interactions at alternative sites will be negligible.[138,139] Therefore, in our analysis, we consider mutations of only those CcP residues that are located in or around the crystallographic binding site and for which changes in the binding energy have been reported (Figure 3.1c, bold and open labels). As can be seen from Table 3.2, in addition to Cc R13, there appear to be two other hot-spot residues: Cc A81 and CcP V197. Although $\Delta\Delta G_B$ for an unconventional A81G Cc mutation is slightly below the 2 kcal mol^{-1} threshold, we tentatively classify A81 as part of a hot spot in the transient Cc–CcP complex. Interestingly, Cc A81 and CcP V197 exhibit a large coupling energy ($\Delta\Delta G_c$= −1.9±0.7 kcal mol^{-1}), which confirms their importance for protein–protein association[143].

Table 3.2. Effects of surface mutations on Cc–CcP binding

Cc	$\Delta\Delta G_B$ (kcal mol^{-1})	CcP	$\Delta\Delta G_B$ (kcal mol^{-1})	CcP	$\Delta\Delta G_B$ (kcal mol^{-1})
T12A[a]	− 1.3 ± 0.1	E32Q[b]	0.6 ± 0.4	V197A[c]	2.1 ± 0.2
R13A[d]	2.1 ± 0.2	D34A[c]	− 0.9 ± 0.7	D217A[c]	0.4 ± 0.2
K72A[c]	0.3 ± 0.2	D34N[b]	0.8 ± 0.4	E290A[c]	6.2 ± 0.2[e]
A81G[c]	1.9 ± 0.4	E35Q[b]	0.7 ± 0.3	E290N[b]	0.9 ± 0.3
K87A[c]	0.9 ± 0.2	Y39A[d]	1.6 ± 0.2	E291N[b]	− 0.1 ± 0.3

[a] Dr. A. N. Volkov, personal communication; experimental conditions are the same as in the present study.

[b] The data, taken from Erman et al., are for binding of horse Cc (*I* = 50 mM; 298 K, pH 6.0).[142]

[c] Taken from Pielak and Wang (*I* = 82 mM; 298 K, pH 6.0).[143]

[d] This work (*I* = 125 mM; 303 K, pH 6.0).

[e] The reported value is most likely erroneous and is disregarded in our analysis.

It should be noted that the traditional hot-spot cutoff $\Delta\Delta G_B$=2 kcal mol^{-1} originates from analyses of strong protein interactions[129-132] and constitutes only a small fraction of

the total binding energy in tight static complexes (e.g., 12–16% for systems with K_d in the picomolar to nanomolar range). For weak transient interactions, this fraction will be larger (e.g., 27% for the protein complex studied here). If, correspondingly, the cutoff value for Cc–CcP analysis is decreased to 1–1.5 kcal mol^{-1}, the binding hot spot will also include CcP Y39 (Table 3.2).

Given the location of two energetically important Cc residues (R13 and A81; Figure 3.1b), it appears that the Cc hot spot encompasses the region around the haem group. We suggest that other haem neighbors such as Q16, V28, and F82, which would be prime targets for further mutagenesis, could also be part of the hot spot. Similarly, the residues surrounding the energetically important CcP V197 side chain (e.g., A194, N195, N196, and Q120; Figure 3.1c) could form the corresponding hot-spot region on the CcP surface. Interestingly, it has been shown recently that Cc residues T12, R13, V28, and A81 form a binding core in complex with cytochrome bc_1 and determine the specificity of the interaction.[159]Notably, mutations of the peripheral interfacial residues on both Cc (K72 and K87) and CcP (E32, D34, and E35) have very little influence on protein binding (Table 3.2 and Figure 3.1b and c). Likewise, alanine substitutions of CcP amino acids located outside of the binding interface (Figure 3.1c, open labels) have no effect on the complex formation, confirming that the binding geometry observed in the crystal structure persists in the solution complex. Taken at face value, our findings support the O-ring hypothesis, which predicts the energetic unimportance of the side-chain groups surrounding the hot spot.[129] At the same time, the O-ring residues are believed to seal the binding surface from the solvent;[129] however, the Cc–CcP interface is "wet",[81,160] a situation observed for many protein complexes.[159-162] Thus, it appears that the proposed function of the O-ring might not be universal. An alternative explanation for the neutral effect of alanine mutations of peripheral residues on binding energy is that the sidechain atoms are replaced by water molecules, and that the newly introduced protein–solvent interactions restore binding.[134,161]

Concluding remarks

In this work, we have identified several hot-spot residues in a weak transient complex of Cc and CcP. Although further work is required to accurately delineate the entire hot

spot, our present findings and the results of earlier studies[142,143] allow us to outline the energetically important binding regions on both proteins and suggest the most promising residues for future mutational analysis. Based on the results of Kiel et al.[137] and our preset data, we would like to propose that binding energy hot spots, which are prevalent in static protein complexes,[129,132,135] can also govern transient protein interactions.